Synthesis, Structural and Magnetic Properties of Ternary Complexes of (Me$_4$P$^+$)·{[Fe(I)Pc(−2)]$^-$}·Triptycene and (Me$_4$P$^+$)·{[Fe(I)Pc(−2)]$^-$}·(N,N,N′,N′-Tetrabenzyl-p-phenylenediamine)$_{0.5}$ with Iron(I) Phthalocyanine Anions

Dmitri V. Konarev,*,[†] Manabu Ishikawa,[‡] Salavat S. Khasanov,[§] Akihiro Otsuka,[‡] Hideki Yamochi,[‡] Gunzi Saito,[∥] and Rimma N. Lyubovskaya[†]

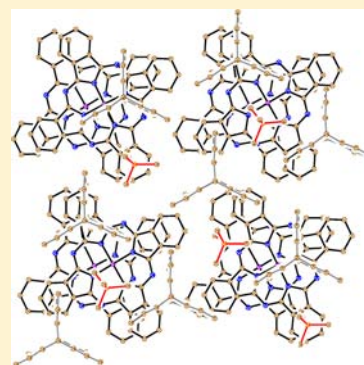[†]Institute of Problems of Chemical Physics RAS, Chernogolovka, Moscow Region, 142432 Russia

[‡]Research Center for Low Temperature and Materials Sciences, Kyoto University, Kyoto 606-8501, Japan

[§]Institute of Solid State Physics RAS, Chernogolovka, Moscow Region, 142432 Russia

[∥]Faculty of Agriculture, Meijo University, 1-501 Shiogamaguchi, Tempaku-ku, Nagoya 468-8502, Japan

S *Supporting Information*

ABSTRACT: Ternary complexes of (Me$_4$P$^+$)·{[Fe(I)Pc(−2)]$^-$}·TPC (**1**) and (Me$_4$P$^+$)·{[Fe(I)Pc(−2)]$^-$}·(TBPDA)$_{0.5}$ (**2**) containing iron(I) phthalocyanine anions, tetramethylphosphonium cations (Me$_4$P$^+$), and neutral structure-forming triptycene (TPC) or N,N,N′,N′-tetrabenzyl-p-phenylenediamine (TBPDA) molecules have been obtained as single crystals. In contrast to previously studied ionic compounds with monomeric [(Fe(I)Pc(−2)]$^-$ anions, the anions form coordination {[Fe(I)Pc(−2)]$^-$}$_2$ dimers both in **1** and **2**, in which a nitrogen atom of one phthalocyanine anion weakly coordinates to the iron(I) atom of neighboring [Fe(I)Pc(−2)]$^-$. The Fe···N distances in the dimers are 3.08(1) and 3.12(1) Å in **1** at 280 K and 2.986(5) (100 K) and 3.011(5) Å (180 K) in **2**. The {[Fe(I)Pc(−2)]$^-$}$_2$ dimers are packed in the layers in **1** arranged parallel to the ac plane and in isolated chains in **2** arranged along the a axis. Extended Hückel based calculation of intermolecular overlap integrals showed stronger and weaker π−π interactions within and between phthalocyanine dimers, respectively, both in **1** and **2**. EPR signals of both complexes manifest two components. An major low-field asymmetric component is attributed to the Fe(I) atoms with the d^7 configuration. An origin minor narrow signal with g-factor close to the free-electron value (g = 2.0018−2.0035) is assigned to partial electron density transfer from the iron(I) center to the phthalocyanine macrocycle and the formation of the [Fe(II)Pc(−3)]$^-$ species. Effective magnetic moments of the complexes of 1.69 (**1**) and 1.76 μ_B (**2**) correspond to the contribution of about one S = $^1/_2$ spin per formula unit in accordance with low-spin state of [Fe(I)Pc(−2)]$^-$. Negative Weiss temperatures of −7.6 K (**1**) and −13 K (**2**) in the 30−300 K range indicate antiferromagnetic interaction of spins in the phthalocyanine dimers. The multicomponent approach was previously proposed for the anionic fullerene complex formation. It also seems very promising to design and synthesize anionic phthalocyanine complexes with one- and two-dimensional macrocycle arrangements.

INTRODUCTION

Metal phthalocyanines are promising compounds for the development of optical, conducting, and magnetic materials.[1] Conducting compounds were obtained by chemical and electrochemical oxidation of metal-free and metal-containing phthalocyanines[1b] and by electrochemical oxidation of the [M(III)Pc(−2)(CN)$_2$]$^-$ anions.[1c] Magnetic compounds were prepared by oxidation of manganese(II) phthalocyanine or butoxy-substituted manganese(II) naphthalocyanine by tetra-cyanoethylene (TCNE).[1d,e] It should be noted that functional phthalocyanine compounds were obtained mainly by oxidation.

Some theoretical and experimental works showed that anionic phthalocyanines can also show conducting and magnetic properties. For example, metallic conductivity or even superconductivity is predicted for electron doped nontransition metal phthalocyanines like Mg(II)Pc(−2) and Zn(II)Pc(−2).[2] Recently we have obtained charge transfer complex containing iron(I) phthalocyanine anions with metallocene cations, {[Fe(I)Pc(−2)]$^-$}·(Cp*$_2$Cr(III)$^+$)·(C$_6$H$_4$Cl$_2$)$_4$ (Cp*$_2$Cr: decamethylchromocene). The [Fe(I)Pc(−2)]$^-$ and Cp*$_2$Cr(III)$^+$ ions alternate in the chains and the complex exhibits ferrimagnetic properties.[3] Although phthalocyanine anions are chemically and electrochemically available,[4] information on anionic phthalocyanine compounds in the solid state is very scarce.[5] One of the reasons for this situation is the high air and moisture sensitivity of phthalocyanine anions due to negative reduction potentials of phthalocyanines ($E^{0/−}$
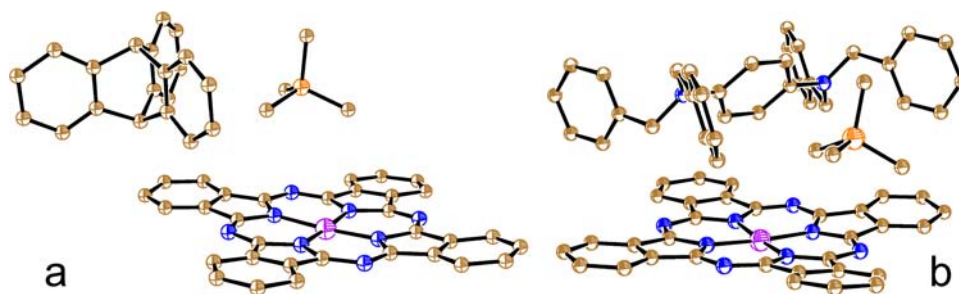
Figure 1. Molecular structure of iron(I) phthalocyanine anions, tetramethylphosphonium cations, and neutral structure-forming TPC and TBPDA molecules in **1** (a) and **2** at 180(1) K (b).

of Fe(II)Pc(−2), Ni(II)Pc(−2), Zn(II)Pc(−2) is equal to −0.70 to −0.78 V versus SCE in noncoordinating 1-methylnaphthalene at 150 °C[6]). At present, anionic metal phthalocyanines in solid state are mainly obtained by doping with alkali metals in gaseous phase.[7] This method has not allowed the preparation of single crystals. Therefore, the development of new synthetic approaches for the preparation of single crystals of anionic phthalocyanine compounds is important.

Previously we developed a multicomponent approach to prepare anionic fullerene complexes.[8] This strategy was very fruitful in the synthesis of the complexes with one- and two-dimensional packing of fullerene anions.[9] In this case two donor components are cocrystallized with fullerene to form the $(D_1^+)\cdot(C_{60}^{\bullet-})\cdot(D_2)$ complexes. The D_1^+ component is a small cation or donor whose electron donating properties are strong enough to generate fullerene anions, whereas the D_2 component remains neutral and defines the crystal packing of the complex due to large size of the molecule. Different organic molecules can be used as D_2 components.[8] For example, neutral triptycene (TPC) molecules form hexagonal network able to accommodate small cations such as N-methyldiazabicyclooctane cation (MDABCO$^+$). At the same time a hexagonal TPC network becomes a template to arrange fullerene anions in closely packed hexagonal layers. As a result, the $(MDABCO^+)\cdot(C_{60}^{\bullet-})\cdot$TPC complex manifests quasi-two-dimensional metallic conductivity.[9g] Another organic molecule N,N,N′,N′-tetrabenzyl-p-phenylenediamine (TBPDA) forms a series of ternary $(D_1^+)\cdot(C_{60}^{\bullet-})\cdot$(TBPDA) complexes, where D_1^+ can be tetrakis(dimethylamino)ethylene (TDAE$^+$), Cp$^*_2$Cr(III)$^+$, or decamethylcobaltocene (Cp$^*_2$Co(III)$^+$). These complexes are not conducting and manifest only weak antiferromagnetic interaction of spins due to large spatial separation of paramagnetic D_1^+ and $C_{60}^{\bullet-}$ ions by diamagnetic TBPDA molecules.[9a,b]

This report describes the first application of the multicomponent approach to synthesize anionic phthalocyanine compounds. We selected iron(II) phthalocyanine since it is more easily reduced as compared with other phthalocyanines of first-row transition metals.[7] To obtain salts with anionic phthalocyanines we developed a new simple and convenient method for the reduction of metal phthalocyanines in solution. On the basis of our experience in the design of multicomponent complexes of fullerenes,[9a,b,g] we introduced neutral organic triptycene (TPC) and N,N,N′,N′-tetrabenzyl-p-phenylenediamine (TBPDA) molecules into the ionic $\{Me_4P^+\}-\{[Fe(I)Pc(−2)]^-\}$ composition. As a result, two complexes $(Me_4P^+)\cdot\{[Fe(I)Pc(−2)]^-\}\cdot$TPC (**1**) and $(Me_4P^+)\cdot\{[Fe(I)Pc(−2)]^-\}\cdot$(TBPDA)$_{0.5}$ (**2**) have been obtained as single crystals.

In contrast to previously studied ionic compounds $\{[Fe(I)-Pc(−2)]^-\}\cdot($cryptand[2,2,2]$\cdot[M^+])\cdot$solvent ($M^+$ = Na$^+$, K$^+$, solvent = $C_6H_4Cl_2$) and $(C_{70}^-)_2\cdot\{[Fe(I)Pc(−2)]^-\}_6\cdot($cryptand-[2,2,2]$\cdot[Na^+])_8\cdot$solvent containing monomeric $[Fe(I)Pc(−2)]^-$ anions,[5a,c] the $[Fe(I)Pc(−2)]^-$ anions are dimerized both in **1** and **2** to form one- and two-dimensional structures, respectively. The coexistance of major $[(Fe(I)Pc(−2)]^-$ and minor $[(Fe(II)Pc(−3)]^-$ states is demonstrated.

■ RESULTS AND DISCUSSION

a. Synthesis. There are many reports about the study of iron(I) phthalocyanine anions in solution,s[10] but only several salts were isolated and structurally characterized in solid state. Iron(I) phthalocyanine anions can be generated in solution by reduction of Fe(II)Pc(−2) by strong donors like decamethylchromocene.[3] Salts of $[Fe(I)Pc(−2)]^-$ with potassium or sodium cryptand[2,2,2] and the salt of $[Fe(I)Pc(−3)]^{2-}$ with lithium crown ether can be obtained by the reduction of Fe(II)Pc(−2) with alkali metals or sodium fluorenone in the presence of cryptands and crown ethers.[5a,c] Recently we have obtained an unusual salt containing simultaneously planar iron(I) phthalocyanine anions and dumbbell-shaped negatively charged $(C_{70}^-)_2$ dimers.[5c]

We developed a new simple method to generate iron(I) phthalocyanine anions in solution. Fe(II)Pc(−2) is reduced by an excess of zinc dust in the presence of the salts with organic cations (Me$_4$P$^+$, Et$_4$N$^+$, and so on) in hot o-dichlorobenzene/benzonitrile mixture (14:3) at 170−180 °C in anaerobic conditions. Reduction of Fe(II)Pc(−2) is finished within 15−20 min monitored by complete disappearance of solid Fe(II)Pc(−2) and the formation of violet solution containing $[Fe(I)Pc(−2)]^-$. This method is also suitable for the generation of cobalt(I) phthalocyanine anions in solution. Iron(I) phthalocyanine salts with small cations are insoluble in pure o-dichlorobenzene at room temperature. Addition of benzonitrile into the reaction mixture makes these salts soluble, and they can be precipitated or crystallized by slow diffusion of hexane.

We found that in most cases iron(I) phthalocyanine salts with small cations do not crystallize (only powders were obtained). In the case of anionic C_{60} complexes, the crystalline ternary $(D_1^+)\cdot(C_{60}^{\bullet-})\cdot(D_2)$ complex can be obtained even when the corresponding two-component $(D_1^+)\cdot(C_{60}^{\bullet-})$ complex does not form stable crystals.[8] We tried to prepare ternary complexes of phthalocyanines by adding organic compounds into the solution containing $[Fe(I)Pc(−2)]^-$ and Me$_4$P$^+$ ions followed by the crystallization with the aid of hexane. Good small plate-like crystals of dark gold color were obtained on the walls of the diffusion cell when TPC and TBPDA were

examined, respectively. Crystals were investigated by X-ray diffraction, optical, EPR, and SQIUD techniques. Compositions of crystals determined from X-ray diffraction data were found to be $(Me_4P^+)\cdot\{[Fe(I)Pc(-2)]^-\}\cdot TPC$ (**1**) and $(Me_4P^+)\cdot\{[Fe(I)-Pc(-2)]^-\}\cdot(TBPDA)_{0.5}$ (**2**). Mainly on the basis of the magnetic properties, the formal charge of each constituent was derived as shown here, which includes the open-shell monoanion, $[Fe(I)Pc(-2)]^-$. Several crystals obtained from the different batches showed the same unit cell parameters and molecular structures for each salt (Figure 1 a,b).

b. Optical Properties of 1 and 2. Complexes **1** and **2** show strong absorption in the vis−NIR range which can unambiguously be attributed to the $[Fe(I)Pc(-2)]^-$ anions. The bands are observed at 821, 688, 554, 528, 487, 445, 325 nm in the spectrum of **1** and at 817, 686, 553, 532, 482, 440, and 322 in the spectrum of **2** (Figure 2). $\{[Fe(I)-$
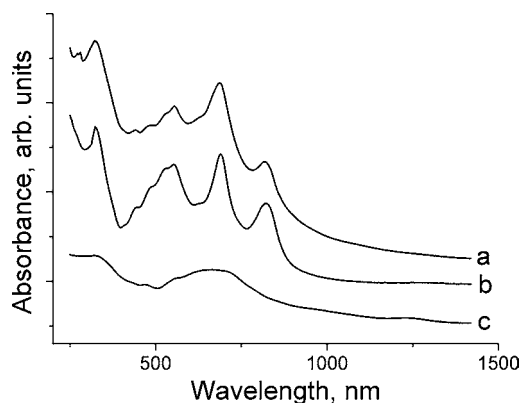
Figure 2. Spectra of **1** (a), **2** (b), and starting Fe(II)Pc(−2) (c) in the UV−vis−NIR ranges measured in KBr pellets.

$Pc(-2)]^-\}\cdot(cryptand[2,2,2]\cdot[Na^+])\cdot(C_6H_4Cl_2)$ and $(C_{70}^-)_2\cdot\{[Fe(I)Pc(-2)]^-\}_6\cdot(cryptand[2,2,2]\cdot[Na^+])_8\cdot$solvent salts containing isolated $[Fe(I)Pc(-2)]^-$ anions show similar spectra.[5c] The spectra of $[Fe(I)Pc(-2)]^-$ in **1** and **2** are noticeably different from that of neutral Fe(II)Pc(−2) having only one broad band in the visible range with maximum at 662 nm (Figure 2c).

The IR spectrum of Fe(II)Pc(−2) remains almost unchanged at the formation of the $[(Fe(I)Pc(-2)]^-$ anions in **1** and **2**. Only several bands are shifted by 1−5 cm^{-1}, and some weak bands disappear (see Supporting Information). Most probably, the geometry of phthalocyanine macrocycle is retained at the formation of the complexes since negative charge on $[Fe(I)Pc(-2)]^-$ is mainly localized on the iron(I) atoms.

c. Crystal Structures of 1 and 2. Both complexes have monoclinic lattices with $P2_1/c$ and $P2_1/n$ space groups for **1** and **2**, respectively. All components are well ordered. Complex **1** contains two each of crystallographically independent $[Fe(I)Pc(-2)]^-$, Me_4P^+, and TPC, whereas complex **2** contains only one crystallographically independent $[Fe(I)Pc(-2)]^-$ and Me_4P^+ and half of the TBPDA molecule. The lengths of the Fe−N(Pc) bonds in FePc are nearly insensitive to spin state of the central iron atom and charge state of phthalocyanine since the Fe−N(Pc) bonds in low-spin $Fe(II)Pc\cdot(Py)_2$ $(S = 0)$,[12] neutral Fe(II)Pc with intermediate $(S = 1)$ spin state,[11] and the $[Fe(I)Pc(-2)]^-$ anions in $\{[Fe(I)Pc(-2)]^-\}\cdot(cryptand-[2,2,2]\cdot[Na^+])\cdot C_6H_4Cl_2$ have close lengths (Table 1).[5c] The average Fe−N(Pc) bond lengths were 1.91(1) Å at 280 K in **1**, and 1.920(4) and 1.919(3) Å in **2** at 100 and 180 K, respectively.

An interesting peculiarity of both complexes is the formation of $\{[Fe(I)Pc(-2)]^-\}_2$ dimers (Figure 3 shows dimers in **2** at 180 K). The dimers are organized such a way that nitrogen atom of one $[Fe(I)Pc(-2)]^-$ is arranged over the iron(I) atom of neighboring $[Fe(I)Pc(-2)]^-$. The Fe···N distances of 3.08(1) and 3.12(1) Å are formed in **1** at 280 K and 2.986(5) Å (100 K) and 3.011(5) Å (180 K) in **2** indicating weak coordination of neighboring phthalocyanine to the iron(I) atom. The presence of weak coordination is supported by a noticeable displacement of iron(I) atoms from the plane of four nitrogen atoms and the 24-atom phthalocyanine plane by 0.070−0.076 and 0.120−0.154 Å, respectively, toward coordinated nitrogen atoms (Table 1). Thus, in contrast to previously studied isolated $[Fe(I)Pc(-2)]^-$ anions which contain four-coordinated iron(I) atoms,[5c] the iron(I) atoms in **1** and **2** form four strong equatorial Fe−N bonds and one weak axial Fe−N bond. The formation of the $\{[Fe(I)Pc(-2)]^-\}_2$ dimers affects

Table 1. Geometry of FePc at Different Coordination and Charge State

compound		charge	spin state of Fe	lengths of Fe−N(Pc) bonds/av d value, Å	displacement of Fe(I) atoms from 4N- and 24-atom plane {in braces}, Å	Fe−N distance in dimers, Å	ref
Fe(II)Pc(−2)	293 K	0	$S = 1$	1.926(1)	0		11
Fe(II)Pc(−2)	301 K	0	$S = 1$	1.925(2)	0		this work
Fe(II)Pc(−2)	100 K	0	$S = 1$	1.926(1) 1.927(1)	0		this work
Fe(II)Pc(−2)·(Py)$_2$	293 K	0	$S = 0$	1.939(2) 1.938(2)/ 1.938(2)	0		12
$\{[Fe(I)Pc(-2)]^-\}\cdot$ (cryptand[2,2,2]·[Na$^+$])·C$_6$H$_4$Cl$_2$	130 K	−1	$S = 1/2$	1.917(1) 1.919(1)/ 1.918(1)	0		5c
				1.914(1) 1.914(1)/ 1.914(1)	0		
(Me$_4$P$^+$)·$\{[Fe(I)Pc(-2)]^-\}\cdot$ TPC (**1**)	280 K	−1	$S = 1/2$	averaged 1.91(1)	0.07 {0.12}	3.08(1)	this work
						3.12(1)	this work
(Me$_4$P$^+$)·$\{[Fe(I)Pc(-2)]^-\}\cdot$ (TBPDA)$_{0.5}$ (**2**)	180 K	−1	$S = 1/2$	1.929(3), 1.907(3), 1.909(3), 1.932(3)/ 1.919(3)	0.072 {0.151}	3.011(5)	this work
	100 K			1.911(4), 1.912(4), 1.929(4), 1.930(4)/ 1.920(4)	0.076 {0.154}	2.986(5)	this work
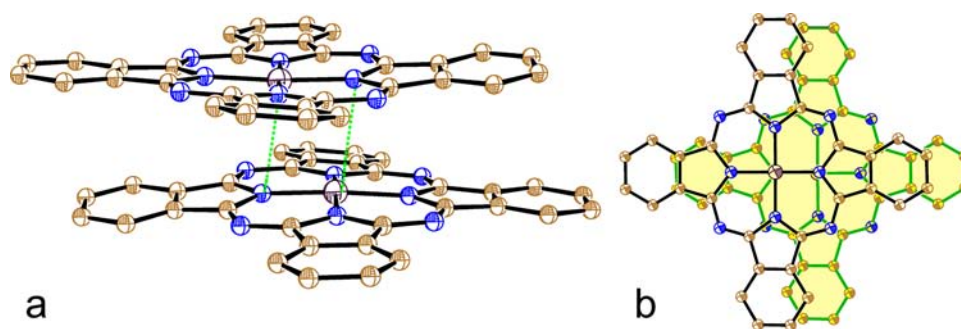
Figure 3. Coordination dimer formed by iron(I) phthalocyanine anions in **2** at 180(1) K: (a) side view (short Fe−N(Pc) distances are shown by green dashed lines); (b) overlapping mode for two [Fe(I)Pc(−2)]⁻ anions in the dimer. Dimers in **1** show similar geometry.
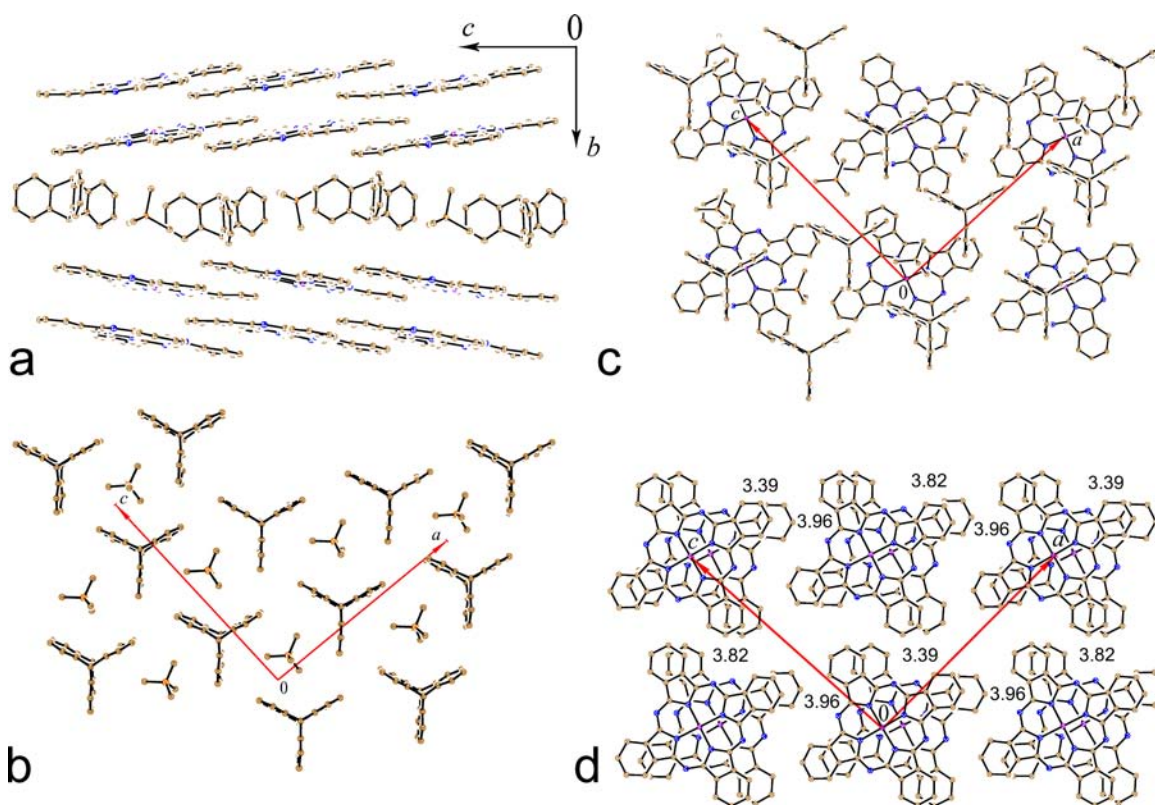

Figure 4. Crystal structure of **1**: (a) view of the phthalocyanine and the Me_4P^+-TPC layers along the *a* axis; (b) view of organic Me_4P^+-TPC layer projected along the *b* axis; (c) projection of the Me_4P^+-TPC layer on negatively charged phthalocyanine layer along the *b* axis (only the top phthalocyanine in each dimer is shown); (d) view of the phthalocyanine layer along the *b* axis (numbers show shortest C···C contacts between the $\{[Fe(I)Pc(-2)]^-\}_2$ dimers).

not only the crystal packing of both complexes but most probably changes the distribution of electron density in the [Fe(I)Pc(−2)]⁻ anions (see section describing Magnetic Properties of **1** and **2**). Dimeric packing is also characteristic of metal porphyrin complexes. For example, octaethylporphyrins of zinc(II), cobalt(II), and iron(II) in the fullerene complexes form dimers with weak coordination of porphyrin nitrogen atom to the metal centers.[13] The Fe−N distances in the $\{Fe(II)OEP(-2)\}_2$ dimers formed in the complex with C_{60} are 3.048 and 3.114 Å.[13c]

The structural feature of **1** is represented as a layered structure (Figure 4a). Neutral triptycene molecules form a hexagonal network with voids which can accommodate small organic cations. For example, voids in the TPC network are occupied by the (MDABCO⁺) cations in previously studied (MDABCO⁺)·($C_{60}^{•-}$)·TPC complex. In this case, the (MDAB-

CO⁺)-TPC layers play the role of a template to build unique hexagonal fullerene layers. Distances between the centers of hexagonal voids in the (MDABCO⁺)-TPC layer are from 9.91 to 10.02 Å. Since these distances are slightly shorter than the van der Waals diameter of C_{60} (10.18 Å), fullerenes are densely packed in the layers.[9g] A similar scheme works at the formation of $(Me_4P^+)·\{[Fe(I)Pc(-2)]^-\}·TPC$ (**1**). The Me_4P^+ cations also fit well to the hexagonal voids in the TPC network (Figure 4b). The (Me_4P^+)-TPC layers are arranged in the *ac* plane with distances between the centers of the hexagonal voids in the 9.64−10.34 Å range. As a result, phthalocyanine dimers also form layers in the *ac* plane. By analogy with fullerene complex we could expect that the structure of the (Me_4P^+)-TPC layers can define the packing motif of phthalocyanine layers. However, this effect is not dominant due to phthalocyanines
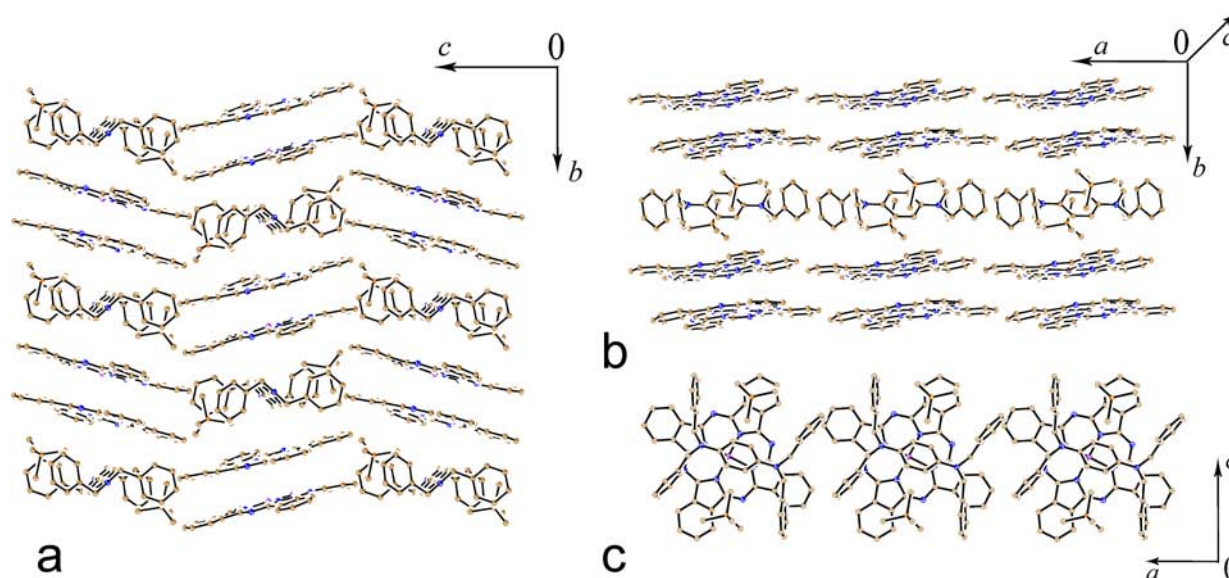
Figure 5. Crystal structure of **2** at 180(1) K: (a) view along the chains from the $\{[Fe(I)Pc(-2)]^-\}_2$ dimers and the *a* axis; (b) view showing chains of the $\{[Fe(I)Pc(-2)]^-\}_2$ dimers alternating with the TBPDA and Me_4P^+ species; (c) projection the TBPDA and Me_4P^+ components on the chain from the $\{[Fe(I)Pc(-2)]^-\}_2$ dimers (view along the *b* axis).

have larger size (approximately 16.2 Å) in comparison with the period of TPC network (approximately 10 Å) (Figure 4c).

Phthalocyanines have nearly square shape of the molecules. As a result, the $\{[Fe(I)Pc(-2)^-\}_2$ dimers are also packed in square layers with distances between the central iron(I) atoms in the 12.8−13.6 Å range (Figure 4d). Although the $\{[Fe(I)Pc(-2)]^-\}_2$ dimers are closely packed in the layers, there is no strong π−π interaction between them since only several side-by-side C···C contacts are formed (Figure 4d). Multiple H(TPC, Me_4P^+)···C,N$\{[Fe(I)Pc(-2)]^-\}$ contacts are formed between TPC, Me_4P^+, and $[Fe(I)Pc(-2)]^-$ in the 2.66−2.96 Å range. Each Me_4P^+ cation is surrounded by three TPC molecules and in total 12 close H(Me_4P^+)···C(TPC) contacts are formed between them in the 2.50−3.00 Å range.

The main structural motif of **2** is chains formed by the $\{[Fe(I)Pc(-2)]^-\}_2$ dimers arranged along the *a* axis (Figure 5b). These chains alternate with the $(Me_4P^+)_2$·TBPDA units along the *b* and *c* axes (Figures 5a). There are close van der Waals C···C contacts between the $\{[Fe(I)Pc(-2)]^-\}_2$ dimers in the chains of about 3.50 Å length, whereas these chains are well separated from each other (shortest C···C distance between the $\{[Fe(I)Pc(-2)]^-\}_2$ dimers from the neighboring chains exceed 6 Å). TBPDA molecules are arranged over the central part of phthalocyanine macrocycle, and two Me_4P^+ cations are located close to the phenylene groups of phthalocyanine (Figure 5c). Multiple H(TBPDA, Me_4P^+)···C, N, Fe$\{[Fe(I)Pc(-2)]^-\}$ and two C(TBPDA, Me_4P^+)···C$\{[Fe(I)Pc(-2)]^-\}$ contacts are formed between them in the 2.50−2.86 and 3.46−3.48 Å range, respectively. Since TBPDA molecule encapsulates two Me_4P^+ cations between benzyl substituents, many H-(Me_4P^+)···C(TBPDA) contacts are formed in the 2.68−2.90 Å range.

d. Molecular Orbital Calculations for the Complexes. The electronic structure and the intermolecular overlap integrals in **1** and **2** were examined by an extended Hückel method[14] based on the results of X-ray single crystal structure analyses. The interactions between FePc skeletons were evaluated by overlap integrals among the frontier orbitals of them (LUMOs for $[Fe(I)Pc(-2)]^-$ or SOMOs for $[Fe(II)$-

$Pc(-3)]^-$, see the section e). As we discussed in the crystal structure section, the $[Fe(I)Pc(-2)]^-$ anions form coordination $\{[Fe(I)Pc(-2)]^-\}_2$ dimers, and these dimers are packed in the layers in **1** and chains in **2**. Two types of interactions exist between phthalocyanines, namely, relatively strong intradimer π−π interaction and weaker interdimer interaction. Intradimer overlap integrals in **2** are bigger than that in **1** (Table 2). That

Table 2. Intra- and Interdimer Overlap Integrals Calculated for 1 and 2[a]

temp	intradimer overlap integrals, 10^{-3}	interdimer overlap integrals, 10^{-3}
$(Me_4P^+)\cdot\{[Fe(I)Pc(-2)]^-\}\cdot TPC$ (**1**)		
280 K	−4.9	$s1 = -0.2, s2 = s3 = -0.1$
$(Me_4P^+)\{[Fe(I)Pc(2)]^-\}(TBPDA)_{0.5}$ (**2**)		
180 K	7.5	$s1 = s2 = 0.1$
100 K	−7.9	$s1 = -0.1$

[a]Overlap integrals are labeled according to Figure 6.

agrees with essentially shorter interplane distances between phthalocyanines in the dimers of **2** (the Fe···N distances are 2.986(5) Å (100 K) and 3.011(5) Å (180 K)) as compared with those in **1** (the Fe···N distances are 3.08(1) and 3.12(1) Å at 280 K). Interdimer overlap integrals in **1** are nonzero for three neighboring phthalocyanine dimers (Table 2, Figure 6a) indicating that this compound has two-dimensional layered packing of phthalocyanines in spite of their magnitude being relatively small as compared with those in metallic and highly conducting one-dimensional conductors based on the [Co-(III)Pc(-2)(CN)$_2$]$^-$ and [Fe(III)Pc(-2)(CN)$_2$]$^-$ anions $(2.7-10 \times 10^{-3})$.[1c,d,15] Interdimer overlap integrals in **2** are of a similar magnitude to those in **1** but serve only in chains. It is also seen that interdimer overlap integrals increase with distances between phthalocyanine planes in the dimers (interdimers overlap integrals in **1** are bigger than those in **2**).

The control of relative mangnitudes of intra- and interdimer interactions and the dimensionality of interdimer interactions are subjects to be solved in the future by applying a multicomponent approach.
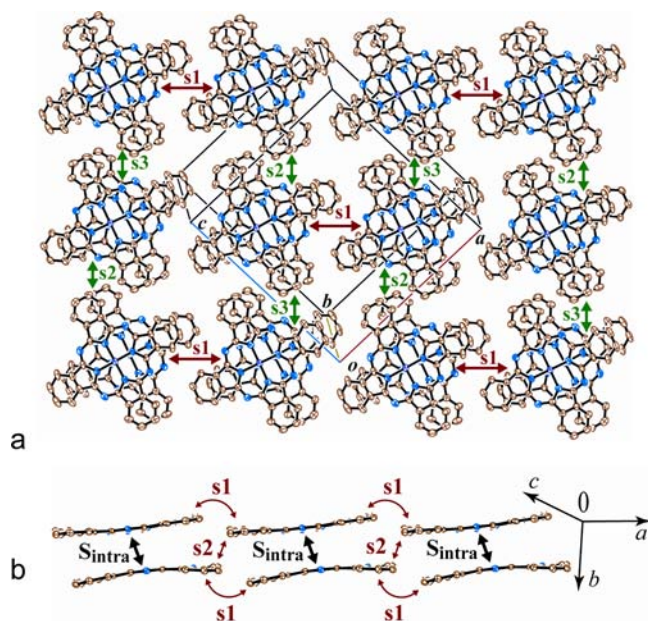
Figure 6. Overlap integrals: (a) for the layers consisting of the $\{[Fe(I)Pc(-2)]^-\}$ dimers in **1** at 280 K; (b) for the chains consisting of the $\{[Fe(I)Pc(-2)]^-\}$ dimers in **2** at 180 K.

e. Magnetic Properties of 1 and 2. EPR spectra of the complexes are shown in Figure 7. Each complex manifested an asymmetric intense low-field signals and a symmetric narrow line at higher field. An asymmetric signal in **1** can be fitted by two lines beginning from room temperature (RT) down to about 100 K (marked by g_1 and g_2 in Figure 7a). The parameters of these lines are $g_1 = 2.1156$ and line width (ΔH) of 88.2 mT and $g_2 = 2.1075$ ($\Delta H = 28.3$ mT). The signal becomes even more asymmetric below 100 K, and it can be fitted by three lines. The third line appears at $g_3 = 2.4312$ ($\Delta H = 14.0$ mT). A low-field EPR signal in **2** is also asymmetric and can be fitted by two lines in the 130−295 K range ($g_1 = 2.5382$ (ΔH) of 15.4 mT, and $g_2 = 2.2823$ ($\Delta H = 40$ mT) at 150 K, Figure 7b). As in **1**, the signal becomes more asymmetric below 130 K, and fitting can be made only by three lines with $g_1 = 2.5463$ ($\Delta H = 16.4$ mT), $g_2 = 2.2700$ ($\Delta H = 29.6$ mT), and $g_3 = 2.0849$ ($\Delta H = 7.1$ mT) (Figure 7c, spectrum at 24 K is shown). These low-field signals can be attributed to the iron(I) atoms with low-spin d^7 electronic configuration. It is interesting that in previously studied solid salts with isolated $[Fe(I)Pc(-2)]^-$ anions containing four-coordinated iron(I) atoms EPR signals were fitted by only two lines down to 4 K,[5c]

whereas signals are more asymmetric in the spectra of **1** and **2** (130−4 K). Since complexes **1** and **2** contain coordination $\{[Fe(I)Pc(-2)]^-\}_2$ dimers, the increase of asymmetry of the EPR signals can be attributed to the appearance of additional weak axial Fe(I)−N(Pc) coordination in the dimers (Figure 3). Indeed, signal asymmetry increases noticeably in **2** when the axial Fe(I)−N(Pc) bond shortens from 3.011(5) to 2.986(5) Å at the temperature decrease from 180 down to 100 K.

Additional to the asymmetric low-field signals, narrow lines are observed both in the spectra of **1** and **2**. This line has $g_{PC} = 2.0035$ and $\Delta H = 0.76$ mT at RT in the spectrum of **1** (Figure 7a). It is observed in whole studied temperature range from RT down to 4 K, and its intensity is about 6% at RT from that of the low-field signal. Complex **2** manifests narrow line with $g_{PC} = 2.0018$ ($\Delta H = 0.12$ mT) at RT. This line has weaker intensity corresponding to less than 0.5% from that of the low-field signal. To be sure that this is not a signal from impurities we studied EPR spectra of a well-shaped single crystal of **2** and found that both asymmetric low-field signal and narrow line are still observed even for one single crystal almost with the same relative intensities as for a polycrystalline sample. According to g-factor value, which is close to free electron value ($g = 2.0023$), a narrow line both in **1** and **2** can be attributed to the admixture of the $[Fe(II)Pc(-3)]^-$ species in which electron density is localized on the phthalocyanine macrocycle. These species coexist with main $[Fe(I)Pc(-2)]^-$ species with the localization of negative charge on the iron(I) metal. It should be noted that narrow signals are not observed in the salts with isolated $[Fe(I)Pc(-2)]^-$ anions containing four-coordinated iron(I) atoms.[5c] Therefore, the $[Fe(II)Pc(-3)]^-$ admixture most probably appears due to weak coordination of phthalocyanine to the iron(I) center. Previously,[10a] it was found that narrow signals with g-factors close to free electron value are also observed together with the signal from the $[Fe(I)Pc(-2)]^-$ anions when these anions are dissolved in coordinating solvent like dimethyl sulfoxide (DMSO). The $[Fe(I)Pc(-2)]^-$ anions exist in DMSO solution as five-coordinate DMSO·$[Fe(I)Pc(-2)]^-$ species. Six-coordinate $(DMSO)_2·[Fe(II)Pc(-3)]^-$ species with delocalization of negative charge over the phthalocyanine macrocycle are stabilized in coordinating solvents with strong donor strength. Therefore, the following equilibrium exists in solution:[10a]

$$DMSO-[Fe(I)Pc(-2)]^- + DMSO$$
$$\rightleftarrows (DMSO)_2-[Fe(II)Pc(-3)]^-$$
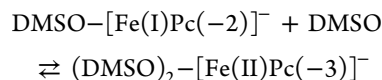
Magnetic properties of **1** and **2** were also studied by SQUID magnetometry. Effective magnetic moments of the complexes
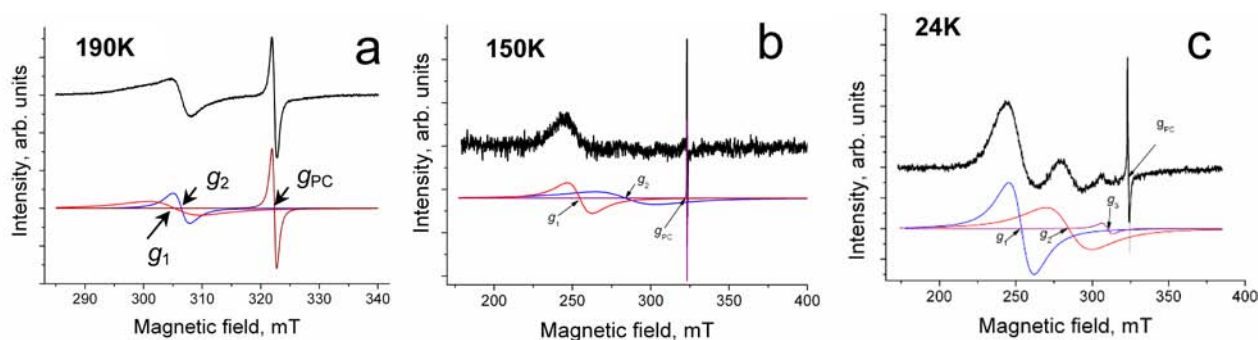
Figure 7. EPR spectra of polycrystalline **1** at 190 K (a), and **2** at 150 K (b) and 24 K (c). For values of g_1, g_2, g_3, and g_{PC}, see text.

are 1.69 (**1**) and 1.74 μ_B (**2**) at 300 K (see Supporting Information). These values correspond to the contribution of about one $S = \frac{1}{2}$ spin per formula unit (the calculated value is $\mu_{eff} = 1.73 \mu_B$) indicating low $S = \frac{1}{2}$ spin state of the $[Fe(I)Pc(-2)]^-$ anions in both complexes. The contribution from the $[Fe(II)Pc(-3)]^-$ admixture to magnetic susceptibility is probably low since in **1** the content of $[Fe(II)Pc(-3)]^-$ does not exceed 6% from that of $[Fe(I)Pc(-2)]^-$ (according to EPR). Temperature dependences of magnetic susceptibility of **1** and **2** follow the Curie−Weiss law with negative Weiss temperatures of −7.6(±0.4) (**1**) and −13(±1) K (**2**) in the 30−300 K range, respectively. The observed temperature dependence of magnetic susceptibility can be fitted well by the Heisenberg model for the pairs of antiferromagnetically interacting spins[16] with $J/k_B = -1.2$ and −1.8 K for **1** and **2**, respectively (see Supporting Information). These values indicate antiferromagnetic interaction of spins localized on $[Fe(I)Pc(-2)]^-$. The overlap integrals within the phthalocyanine dimers are noticeably stronger than those between the dimers. On the basis of these results, we conclude that the observed antiferromagnetic interaction of spins is mainly realized in the $\{[Fe(I)Pc(-2)]^-\}_2$ dimers. Magnetic data are also in a good agreement with the calculations since larger overlap integrals between the $[Fe(I)Pc(-2)]^-$ anions in the phthalocyanine dimers of **2** provide stronger antiferromagnetic interaction between the spins (more negative Weiss temperature and larger J/k_B value). Below 50 K, magnetic transition accompanied by the decrease of effective magnetic moment is possible both in **1** and **2** (see Supporting Information). However, due to the absence of structural data at this temperature it is not possible to discuss the origin of this transition.

CONCLUSIONS

The versatility of the multicomponent approach, which has been applied to provide crystalline fullerene complexes, is proved also to produce single crystalline $[Fe(I)Pc(-2)]^-$ complexes. Two kinds of $[Fe(I)Pc(-2)]^-$ structures were obtained having one- and two-dimensional arrangements of anion species, while both of them contained the anion dimers. The crystallinities of them were good enough to investigate the crystal and physical properties. The partial charge transfer from the Fe(I) atoms to the macrocycle was observed in both cases. Most probably that becomes due to phthalocyanine nitrogen coordination to the Fe(I) atoms in the $\{[Fe(I)Pc(-2)]^-\}_2$ dimers. As a whole, the presented method for the reduction of metal phthalocyanines together with the multicomponent approach opens wide opportunities to develop the field of crystalline anionic phthalocyanine compounds.

EXPERIMENTAL SECTION

a. Materials. Iron phthalocyanine $\{Fe(II)Pc(-2)\}$, triptycene (TPC), tetramethylphosphonium bromide (Me$_4$PBr), and zinc dust were purchased from Aldrich. N,N,N',N'-Tetrabenzyl-p-phenylenediamine (TBPDA) was purchased from Lancaster. These reagents were used without further purification. Solvents were purified in argon atmosphere. o-Dichlorobenzene ($C_6H_4Cl_2$) was distilled over CaH$_2$ under reduced pressure, benzonitrile (C_6H_5CN) was distilled over Na under reduced pressure, and hexane was distilled over Na/benzophenone. The solvents were degassed and stored in a glovebox. All manipulations for the synthesis of air-sensitive **1** and **2** were carried out in a MBraun 150B-G glovebox with controlled atmosphere (O$_2$, H$_2$O < 1 ppm). The crystals were stored in the glovebox and sealed in 2 mm quartz tubes for EPR and SQUID measurements under 10^{-3}

Torr. For IR and UV−vis−NIR measurements, KBr pellets were prepared in the glovebox.

b. Synthesis. Reduction of Fe(II)Pc(−2) (24 mg, 0.042 mmol) by an excess of zinc dust (120 mg) in the presence an excess of Me$_4$PBr (20 mg, 0.16 mmol) was carried out in hot o-dichlorobenzene/benzonitrile mixture (14:3) at 170−180 °C in anaerobic conditions. Reduction was accomplished after 15−20 min with complete dissolution of the phthalocyanine and formation of violet solution of $\{[Fe(I)Pc(-2)]^-\}$. The solution was cooled and filtered. Slow precipitation of the $(Me_4P^+)\cdot\{[Fe(I)Pc(-2)]^-\}$ salt by diffusion of hexane does not result in the formation of any crystals (only black-violet powder was formed). In this case we carried out the preparation of three-component complexes. The obtained solution of $(Me_4P^+)\cdot\{[Fe(I)Pc(-2)]^-\}$ was filtered, and an excess of TPC (150 mg, 0.6 mmol) for **1** or TBPDA (120 mg, 0.626 mmol) for **2** was dissolved over one hour. Solution was filtered into a 50 mL glass tube of 1.8 cm in diameter with a ground glass plug. A 25 mL portion of hexane was layered over the solution. Slow mixing of solvents over 6−8 weeks at room temperature (295 K) yielded the crystals of $(Me_4P^+)\cdot\{[Fe(I)Pc(-2)]^-\}\cdot TPC$ (**1**) and $(Me_4P^+)\cdot\{[Fe(I)Pc(-2)]^-\}\cdot(TBPDA)_{0.5}$ (**2**) on the walls of the tube. The solvent was decanted from the crystals which were then washed with hexane (yield 65% and 22%, respectively). The crystals were very thin dark-gold plates up to 0.1 × 0.1 × 0.02 mm^3 for both **1** and **2**. The composition of the complexes was determined from X-ray structural analysis on a single crystal and was confirmed by elemental analysis for C, H, and N. Several crystals tested from the synthesis had the same unit cell parameters.

Me$_4$P·FePc·TPC (**1**): C$_{56}$H$_{42}$FeN$_8$P (913.80). Found %: C = 73.02, H = 4.24, N = 12.12. Calcd %: C = 73.60, H = 4.60, N = 12.26; P = 3.40; Fe = 6.14.

Me$_4$P·FePc·(TBPDA)$_{0.5}$ (**2**): C$_{53}$H$_{44}$FeN$_9$P (893.79). Found %: C = 70.76, H = 4.62, N = 13.98. Calcd %: C = 71.22, H = 4.92, N = 14.10; P = 3.48; Fe = 6.28.

Single crystals of β-Fe(II)Pc(−2) were grown from purchased Fe(II)Pc(−2) (TCI, >95%). It was sublimed twice under vacuum (10^{-5} Torr) by using temperature gradient sublimation technique. The crystal growth was performed by gradual heating from 420 to 450 °C.

c. General. UV−vis−NIR spectra were measured in KBr pellets on a Perkin-Elmer Lambda 1050 spectrometer in the 250−2500 nm range. FT-IR spectra were measured in KBr pellets with a Perkin-Elmer Spectrum 400 spectrometer (400−7800 cm^{-1}). EPR spectra were recorded from 295 down to 4 K with a JEOL JES-TE 200 X-band ESR spectrometer. A Quantum Design MPMS-XL SQUID magnetometer was used to measure static magnetic susceptibility (χ_M) of **1** and **2** at 100 mT magnetic field in cooling and heating conditions from 300 down to 1.9 K and back from 1.9 up to 300 K. A sample holder contribution and temperature independent core diamagnetic susceptibility (χ_0) were subtracted from the experimental values. The χ_0 value was estimated in the 30−300 K range by the extrapolation of the data in the high-temperature range. Effective magnetic moment (μ_{eff}) was calculated with an appropriate formula: $\mu_{eff} = (8\cdot\chi_M\cdot T)^{1/2}$.

d. X-ray Crystal Structure Determination. *Crystal Data for* **1** *at* 280(1) *K.* C$_{56}$H$_{42}$FeN$_8$P, M_r = 913.80 g mol^{-1}, black plate, monoclinic, $P2_1/c$, a = 18.086(5) Å, b = 25.771(5) Å, c = 19.180(5) Å, β = 93.022(5)°, V = 8927(4) Å^3, Z = 8, d_{calcd} = 1.360 g cm^{-3}, μ = 0.424 mm^{-1}, $F(000)$ = 3800, $2\theta_{max}$ = 43.94°, reflns measured 22 738, unique reflns 10 771, reflns with $I > 2\sigma(I)$ = 2339, params refined 1189, restraints 416, R1 = 0.0819, wR2 = 0.3704, GOF = 0.834, CCDC 906544.

Crystal Data for **2** *at* 180(1) *K.* C$_{53}$H$_{44}$FeN$_9$P, M_r = 893.79 g mol^{-1}, black plate, monoclinic, $P2_1/n$, a = 13.1296(17) Å, b = 12.7055(16) Å, c = 25.672(3) Å, β = 96.672(2)°, V = 4253.5(9) Å^3, Z = 4, d_{calcd} = 1.396 g cm^{-3}, μ = 0.443 mm^{-1}, $F(000)$ = 1864, $2\theta_{max}$ = 52.74°, reflns measured 224 449, unique reflns 8665, reflections with $I > 2\sigma(I)$ = 3173, params refined 581, restraints 0, R1 = 0.0515, wR2 = 0.1087, GOF = 0.714, CCDC 906546.

Crystal Data for **2** *at* 100(1) *K.* C$_{53}$H$_{44}$FeN$_9$P, M_r = 893.79 g mol^{-1}, black plate, monoclinic, $P2_1/n$, a = 13.091(2) Å, b = 12.6449(19) Å, c = 25.604(4) Å, β = 96.535(2)°, V = 4211.0(11) Å^3, Z = 4, d_{calcd} =

1.410 g cm^{-3}, μ = 0.448 mm^{-1}, $F(000)$ = 1864, $2\theta_{max}$ = 49.66°, reflns measured 19 712, unique reflns 7282, reflections with $I > 2\sigma(I)$ = 3119, params refined 581, restraints 0, R1 = 0.0515, wR2 = 0.1385, GOF = 0.754, CCDC 906545.

Crystal Data for β-Fe(II)Pc(−2) at 301(1) K. C$_{32}$H$_{16}$FeN$_8$, M_r = 568.38 g mol^{-1}, black needle, monoclinic, P2$_1$/c, a = 14.602(2) Å, b = 4.7862(7) Å, c = 19.412(3) Å, β = 120.8600(10)°, V = 1164.6(3) Å^3, Z = 2, d_{calcd} = 1.621 g cm^{-3}, μ = 0.691 mm^{-1}, $F(000)$ = 580, $2\theta_{max}$ = 58.56°, reflns measured 13 386, unique reflns 3001, reflns with $I > 2\sigma(I)$ = 2014, params refined 187, restraints 0, R1 = 0.0429, wR2 = 0.1361, GOF = 1.023, CCDC 909994.

Crystal Data for β-Fe(II)Pc(−2) at 100(1) K. C$_{32}$H$_{16}$FeN$_8$, M_r = 568.38 g mol^{-1}, black needle, monoclinic, P2$_1$/c, a = 14.5276(15) Å, b = 4.7810(5) Å, c = 19.185(2) Å, β = 120.7700(10)°, V = 1145.0(2) Å^3, Z = 2, d_{calcd} = 1.649 g cm^{-3}, μ = 0.703 mm^{-1}, $F(000)$ = 580, $2\theta_{max}$ = 58.32°, reflns measured 13 226, unique reflns 2951, reflns with $I > 2\sigma(I)$ = 2396, params refined 187, restraints 0, R1 = 0.0350, wR2 = 0.1111, GOF = 1.111, CCDC 909995.

X-ray diffraction data for **1** at 280(1) K, for **2** at 100(1) and 180(1) K, and for β-Fe(II)Pc(−2) at 100(1) and 301(1) K were collected on an Bruker Smart Apex II CCD with graphite monochromated Mo Kα radiation using an Japan Thermal Engineering Co. cooling system DX-CS190LD. Raw data reduction to F^2 was carried out using Bruker SAINT.[17] The structures were solved by direct method and refined by the full-matrix least-squares method against F^2 using Sir2004.[18] Non-hydrogen atoms were refined in the anisotropic approximation. Positions of hydrogen atoms were calculated geometrically. Subsequently, the positions of H atoms were refined by the "riding" model with U_{iso} = 1.2U_{eq} of the connected non-hydrogen atom or as ideal CH$_3$ groups with U_{iso} = 1.5U_{eq}. Both complexes **1** and **2** are formed as very small and thin plates with maximal size up to 0.1 × 0.1 × 0.02 mm^3. Crystals are very weak diffracting at room temperature, and the reflections are observed only at low angles. The cooling of crystals of **2** down to 180 and 100 K results in the increase in intensity of reflections, and the reflections at higher angles appear allowing this structure to be solved and refined with normal precision. For the crystals of **1**, the number of reflections observed decreases strongly even at very slow cooling, probably due to structural transition. The structure can be solved and refined for the data taken only at 280 K when there are almost no reflections observed at high angles. (There are only 79 reflections observed of the 5494 total number in the shell 0.82 Å < d < 0.95 Å, beyond the limit used for refinement. Even the shell 0.95 Å < d < 1.30 Å comprises only 575 reflections observed of the 6520 total one.) As a result, the ratio of observed/unique reflections and the bond precision are rather low for **1**. Nevertheless, the structure of **1** is solved and refined stably with low residual electron density.

■ ASSOCIATED CONTENT

Ⓢ Supporting Information

Additional table, figures, and crystallographic data in CIF format. This material is available free of charge via the Internet at http://pubs.acs.org.

■ AUTHOR INFORMATION

Corresponding Author

*E-mail: konarev@icp.ac.ru.

Notes

The authors declare no competing financial interest.

■ ACKNOWLEDGMENTS

■ REFERENCES

(1) (b) Inabe, T.; Tajima, H. *Chem. Rev.* **2004**, *104*, 5503. (c) Hasegawa, H.; Naito, T.; Inabe, T.; Akutagawa, T.; Nakamura, T. *J. Mater. Chem.* **1998**, *8*, 1567. (d) Matsuda, M.; Naito, T.; Inabe, T.; Hanasaki, N.; Tajima, H.; Otsuka, T.; Awaga, K.; Narymbetov, B.; Kobayashi, H. *J. Mater. Chem.* **2000**, *10*, 631. (e) Miller, J. S.; Vazquez, C.; Calabrese, J. C.; McLean, M. L.; Epstein, A. J. *Adv. Mater.* **1994**, *6*, 217. (f) Rittenberg, D. K.; Baars-Hibbe, L.; Böhm, A. B.; Miller, J. S. *J. Mater. Chem.* **2000**, *10*, 241. (a) Nyokong, T. *Coord. Chem. Rev.* **2007**, *251*, 1707.
(2) Tosatti, E.; Fabrizio, M.; Tóbik, J.; Santoro, G. E. *Phys. Rev. Lett.* **2004**, *93*, 117002.
(3) Konarev, D. V.; Zorina, L. V.; Khasanov, S. S.; Hakimova, E. U.; Lyubovskaya, R. N. *New J. Chem.* **2012**, *36*, 48.
(4) (a) Taube, R. *Pure Appl. Chem.* **1974**, *38*, 427. (b) Lever, A. B. P.; Milaeva, E. P.; Speier, G. In *Phthalocyanines, Properties and Applications*; Lezuoff, C. C., Lever, A. B. P., Eds.; VCH: New York, 1993; Vol. 3, pp 1−70; (c) Minor, P. C.; Gouterman, M.; Lever, A. B. P. *Inorg. Chem.* **1985**, *24*, 1894.
(5) (a) Tahiri, M.; Doppelt, P.; Fischer, J.; Weiss, R. *Inorg. Chim. Acta* **1987**, *127*, L1. (b) Huckstadt, H.; Homborg, H. *Z. Anorg. Allg. Chem.* **1998**, *624*, 715. (c) Konarev, D. V.; Kuẑmin, A. V.; Simonov, S. V.; Khasanov, S. S.; Otsuka, A.; Yamochi, H.; Saito, G.; Lyubovskaya, R. N. *Dalton Trans.* **2012**, *41*, 13841.
(6) Campbell, R. H.; Heath, G. A.; Hefter, G. T.; McQueen, R. C. S. *J. Chem. Soc., Chem. Commun.* **1983**, 1123.
(7) (a) Margadonna, S.; Prassides, K.; Iwasa, Y.; Taguchi, Y.; Craciun, M. F.; Rogge, S.; Morpurgo, A. F. *Inorg. Chem.* **2006**, *45*, 10472. (b) Taguchi, Y.; Miyake, T.; Margadonna, S.; Kato, K.; Prassides, K.; Iwasa, Y. *J. Am. Chem. Soc.* **2006**, *128*, 3313. (c) Filibian, M.; Carretta, P.; Miyake, T.; Taguchi, Y.; Iwasa, Y. *Phys. Rev. B* **2007**, *75*, 115111.
(8) (a) Konarev, D. V.; Khasanov, S. S.; Lyubovskaya, R. N. *Russ. Chem. Bull.* **2007**, *56*, 371. (b) Konarev, D. V.; Lyubovskaya, R. N. *Russ. Chem. Rev.* **2012**, *81*, 336. (c) Konarev, D. V.; Zorina, L. V.; Khasanov, S. S.; Hakimova, E. U.; Lyubovskaya, R. N. *Russ. Chem. Bull.* **2011**, *60*, 1063. (d) Konarev, D. V.; Zorina, L. V.; Khasanov, S. S.; Lyubovskaya, R. N. *Dalton Trans.* **2012**, *41*, 9170.
(9) (a) Konarev, D. V.; Neretin, I. S.; Saito, G.; Slovokhotov, Yu.L.; Otsuka, A.; Lyubovskaya, R. N. *Dalton Trans.* **2003**, 3886. (b) Konarev, D. V.; Kovalevsky, A.Yu.; Khasanov, S. S.; Saito, G.; Otsuka, A.; Lyubovskaya, R. N. *Eur. J. Inorg. Chem.* **2005**, 4822. (c) Konarev, D. V.; Khasanov, S. S.; Saito, G.; Otsuka, A.; Lyubovskaya, R. N. *J. Mater. Chem.* **2007**, *17*, 4171. (d) Konarev, D. V.; Khasanov, S. S.; Otsuka, A.; Saito, G.; Lyubovskaya, R. N. *Inorg. Chem.* **2007**, *46*, 2261. (e) Konarev, D. V.; Khasanov, S. S.; Otsuka, A.; Saito, G.; Lyubovskaya, R. N. *Dalton Trans.* **2009**, 6416. (f) Konarev, D. V.; Khasanov, S. S.; Mukhamadieva, G. R.; Zorina, L. V.; Otsuka, A.; Yamochi, H.; Lyubovskaya, R. N. *Inorg. Chem.* **2010**, *49*, 3881. (g) Konarev, D. V.; Khasanov, S. S.; Otsuka, A.; Maesato, M.; Saito, G.; Lyubovskaya, R. N. *Angew. Chem.* **2010**, *49*, 4829.
(10) (a) Lever, A. B. P.; Wilshire, J. P. *Inorg. Chem.* **1978**, *17*, 1145. (b) Kaczmarzyk, T.; Jackowski, T.; Dziliński, K. *Nukleonika* **2007**, *52*, S99.
(11) Kirner, J. F.; Dow, W.; Scheidt, W. R. *Inorg. Chem.* **1976**, *15*, 1685.
(12) Janczak, J.; Kubiak, R. *Inorg. Chim. Acta* **2003**, *342*, 64.
(13) (a) Olmstead, M. M.; Costa, D. A.; Maitra, K.; Noll, B. C.; Phillips, S. L.; Van Calcar, P. M.; Balch, A. L. *J. Am. Chem. Soc.* **1999**, *121*, 7090. (b) Ishii, T.; Aizawa, N.; Yamashita, M.; Matsuzaka, H.; Kodama, T.; Kikuchi, K.; Ikemoto, I.; Iwasa, Y. *J. Chem. Soc., Dalton Trans.* **2000**, 4407. (c) Konarev, D. V.; Khasanov, S. S.; Saito, G.; Lyubovskaya, R. N. *Cryst. Growth Des.* **2009**, *9*, 1170.
(14) (a) Whangbo, M.-H.; Hoffmann, R. *J. Am. Chem. Soc.* **1978**, *100*, 6093. (b) Ren, J.; Liang, W.; Whangbo, M.-H. *Crystal and Electronic Structure Analysis Using CAESAR*; Prime Color Software, Inc., 1998. This book can be downloaded free of charge from the website: http://www.PrimeC.com/). Default parameters were used.
(15) (a) Matsuda, M.; Naito, T.; Inabe, T.; Hanasaki, N.; Tajima, H. *J. Mater. Chem.* **2001**, *11*, 2493. (b) Takano, S.; Naito, T.; Inabe, T.

Chem. Lett. **1998**, 1249. (c) Matsuda, M.; Asari, T.; Naito, T.; Inabe, T.; Hanasaki, N.; Tajima, H. *Bull. Chem. Soc. Jpn.* **2003**, *76*, 1935.

(16) Smart, J. S. *Magnetism III*; Rado, G. T., Suhl, H., Eds.; Academic Press: New York, 1963, p 63.

(17) Bruker Analytical X-ray Systems, Madison, WI, 1999.

(18) Burla, M. C.; Carrozzini, B.; Caliandro, R.; Cascarano, G.; Giacovazzo, C.; Polidori, G.; Spagna., R. *Acta Crystallogr., Sect. A* **2003**, *59*, 560.

3859

dx.doi.org/10.1021/ic3025364 | *Inorg. Chem.* 2013, 52, 3851−3859